



Carbon dioxide and methane fluxes at the air–sea interface of Red Sea mangroves

Mallory A. Sea, Neus Garcias-Bonet, Vincent Saderne, and Carlos M. Duarte

King Abdullah University of Science and Technology (KAUST), Red Sea Research Center (RSRC),
Thuwal, 23955-6900, Saudi Arabia

Correspondence: Vincent Saderne (vincent.saderne@kaust.edu.sa)

Received: 18 January 2018 – Discussion started: 31 January 2018

Revised: 16 July 2018 – Accepted: 30 July 2018 – Published: 4 September 2018

Abstract. Mangrove forests are highly productive tropical and subtropical coastal systems that provide a variety of ecosystem services, including the sequestration of carbon. While mangroves are reported to be the most intense carbon sinks among all forests, they can also support large emissions of greenhouse gases (GHGs), such as carbon dioxide (CO₂) and methane (CH₄), to the atmosphere. However, data derived from arid mangrove systems like the Red Sea are lacking. Here, we report net emission rates of CO₂ and CH₄ from mangroves along the eastern coast of the Red Sea and assess the relative role of these two gases in supporting total GHG emissions to the atmosphere. Diel CO₂ and CH₄ emission rates ranged from -3452 to $7500 \mu\text{mol CO}_2 \text{ m}^{-2} \text{ d}^{-1}$ and from 0.9 to $13.3 \mu\text{mol CH}_4 \text{ m}^{-2} \text{ d}^{-1}$ respectively. The rates reported here fall within previously reported ranges for both CO₂ and CH₄, but maximum CO₂ and CH₄ flux rates in the Red Sea are 10- to 100-fold below those previously reported for mangroves elsewhere. Based on the isotopic composition of the CO₂ and CH₄ produced, we identified potential origins of the organic matter that support GHG emissions. In all but one mangrove stand, GHG emissions appear to be supported by organic matter from mixed sources, potentially reducing CO₂ fluxes and instead enhancing CH₄ production, a finding that highlights the importance of determining the origin of organic matter in GHG emissions. Methane was the main source of CO₂ equivalents despite the comparatively low emission rates in most of the sampled mangroves and therefore deserves careful monitoring in this region. By further resolving GHG fluxes in arid mangroves, we will better ascertain the role of these forests in global carbon budgets.

1 Introduction

Mangrove forests, typically growing in the intertidal zones of tropical and subtropical coasts, are highly productive components of coastal ecosystems and adapted to high salinity and anoxic conditions associated with waterlogged sediments. Mangrove forests cover a global estimated area of $137\,760 \text{ km}^2$ (Giri et al., 2011) and are typically constrained by temperature, with greatest biomass and species diversity in the equatorial zone (Alongi, 2012). Mangroves rank among the most threatened ecosystems in the biosphere, with losses estimated at 50 % of their global extent over the past 50 years (Alongi, 2012). These losses affect nearly all mangrove regions but the Red Sea, where mangrove coverage has increased by 12 % over the past 4 decades (Almahasheer et al., 2016).

Loss of mangrove forest represents a loss of valuable ecosystem services, including habitat and nurseries for marine species, coastal protection from erosion due to wave action, and the filtration of harmful pollutants from terrestrial sources (Alongi, 2008), as well as loss of CO₂ sink capacity. Additionally, mangroves can become a source of greenhouse gas (GHG) emissions from disturbed soil carbon stocks (Donato et al., 2011; Alongi, 2014). Hence, mangrove conservation and restoration have been proposed as important components of so-called blue carbon strategies to mitigate climate change (Duarte et al., 2013). Indeed, mangroves are reported to be the most intense carbon sinks among all forests, supporting carbon sequestration rates and organic carbon stocks by as much as 5 times higher than those in terrestrial forests (Donato et al., 2011). While mangrove forests cover less than 1 % of the total coastal ocean area, they contribute to almost 15 % of total carbon sequestration in coastal ecosys-

tems (Alongi, 2012), making mangrove forests highly effective in terms of carbon sequestration per unit area. The management of mangroves to maximize CO₂ removal and subsequent storage is gaining momentum as a cost-effective strategy to mitigate climate change.

However, mangrove forests act as both carbon sinks and sources and have been reported to support large GHG emissions in the forms of CO₂ and CH₄ (Allen et al., 2007; Kristensen et al., 2008a; Chen et al., 2016). Whereas concerns are focused on GHG emissions following mangrove disturbance, estimated at 0.02–0.12 Pg C yr⁻¹ globally (Donato et al., 2011), undisturbed mangrove sediments also support GHG emissions (Purvaja and Ramesh, 2000; Kristensen et al., 2008b; Chauhan et al., 2015). Recent reports specifically highlight the importance of methane in flux estimates, as emissions of CH₄ with a higher global warming potential can offset mangrove carbon burial by as much as 20% (Rosentreter et al., 2018b). Previous studies on GHG emission rates either focus on the soil–atmosphere interface, highlighting substantial flux ranges with mangroves reported to act as negligible (Alongi et al., 2005) to considerable sources (Livesley and Andrusiak, 2012; Chen et al., 2016), or examine net fluxes at the air–sea interface, with few studies in arid systems. Comparisons of carbon sequestration rates between mangrove stands have revealed that climatic conditions play an important role, with mangroves in the arid tropics, such as those in the Red Sea, supporting the lowest carbon sequestration rates (Almahasheer et al., 2017). Likewise, GHG emissions from mangrove forests may vary with climate, with most reported rates to-date derived from the wet tropics (Alongi et al., 2005; Chauhan et al., 2015; Chen et al., 2016). Whereas Red Sea mangroves are considered to play a minor role as CO₂ sinks, their role may be greater than portrayed by low carbon burial rates if they also support very low GHG emissions, thereby leading to a balance comparable to mangroves in the wet tropics.

Here we report air–sea emission rates of CO₂ and CH₄, along with their carbon isotopic composition, from incubations of inundated mangrove sediment cores along the Saudi coast of the Red Sea. We assess the relative role of these two gases in supporting total GHG emissions as well as their fluctuations along the day–night cycle.

2 Materials and methods

2.1 Study area

We sampled seven mangrove forests along the eastern coast of the Red Sea (Fig. 1). We collected triplicate sediment cores by inserting translucent PVC tubes (30.5 cm in height and 9.5 cm in diameter) into mangrove sediments, collecting approx. 20 cm of sediment and a top seawater layer. The overlying water was regularly replaced by fresh seawater from the corresponding station in order to fill the remaining

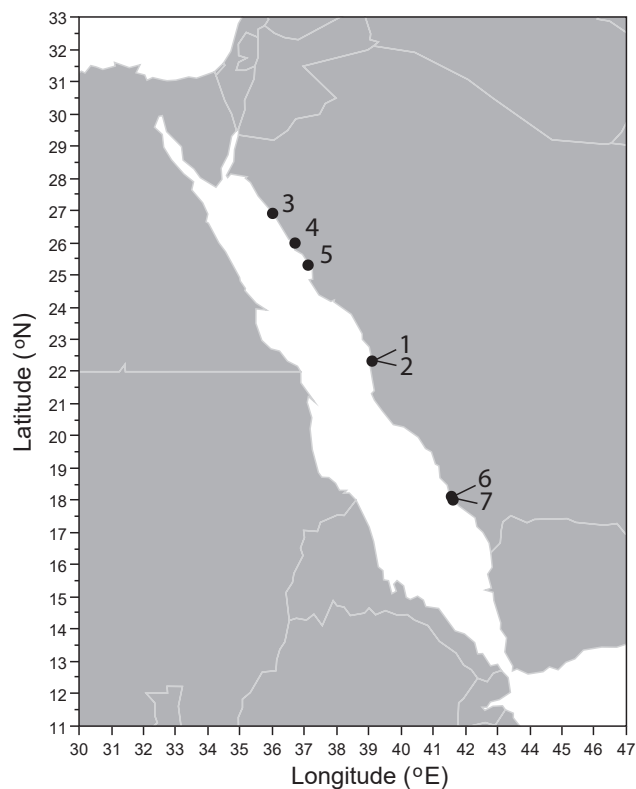


Figure 1. Mangrove stands sampled along the Saudi coast of the Red Sea. Numbers indicate positions of sampling sites from this study. S1 and S2: King Abdullah University of Science and Technology, S3: Duba, S4 and S5: Al Wahj, and S6 and S7: Farasan Banks.

core volume and to measure CO₂ and CH₄ fluxes from underlying sediments during incubations. Mangrove sediments were sampled 5 to 10 m from the forest edge, typically in the centre of the mangrove belt. We sampled two stations (S1 and S2) in January and February 2017 and the other five mangrove stations (S3–S7) in March on board the R/V *Thuwal* as part of a scientific cruise. The cores collected from S1 and S2 were immediately transported to the laboratory, placed in seawater baths and enclosed in environmental growth chambers (Percival Scientific Inc., Perry, IA, USA) with 12:12 light cycles at a constant temperature of 26 °C. The sediment cores collected during the scientific cruise were transported immediately on board and placed in open aquarium tanks with running seawater in order to keep them close to in situ temperature. Salinity and temperature were routinely recorded using a conductivity, temperature, and depth sensor (EXO1, YSI inc., Yellow Springs, USA). Additionally, sediment chlorophyll *a* and nutrient (organic carbon and nitrogen) content was analysed from cores collected during the scientific cruise.

2.2 Sediment characteristics

The chlorophyll *a* content of the sediment was measured by fluorometry. The surface layer of each replicate core was collected and frozen until further analysis. Prior to chlorophyll *a* extraction, the sediment samples were left at room temperature to thaw. The chlorophyll *a* was extracted by adding 7 mL of 90 % acetone to 2 mL of sediment sample. After a 24 h incubation at 4 °C in dark conditions, the samples were centrifuged and the chlorophyll *a* content in the supernatant was measured on a Trilogy fluorometer. The nutrient (organic carbon and nitrogen) content of the sediment was analysed on an Organic Elemental Analyzer (Flash 2000, Thermo Fisher Scientific, Massachusetts, USA) after acidification of sediment samples.

2.3 Measurement of greenhouse gas fluxes

We measured CO₂ and CH₄ air–sea fluxes using two different techniques. The CO₂ and CH₄ fluxes from stations S1 and S2 were measured using the closed water circuit technique and the CO₂ and CH₄ fluxes from the rest of the stations sampled during the scientific cruise (S3–S7) were measured using the headspace technique.

2.3.1 Measurement of CO₂ and CH₄ fluxes in sediment core incubations using closed water circuit technique

We incubated mangrove sediment cores from stations S1 and S2 using a closed water circuit technique in order to measure changes in CO₂ and CH₄ concentrations. Before starting the incubation, the seawater above the sediment from each core was replaced by fresh seawater collected from the same location, avoiding disturbance of the sediment. Then, the seawater from the core was recirculated by a peristaltic pump in an enclosed water circuit through a membrane equilibrator (Liqui-cel mini module, 3M, Minnesota, USA). This set-up enables the equilibration of gases in dissolution with an enclosed air circuit. The air from the enclosed air circuit was then passed through a desiccant column (calcium sulfate, WA Hammond Drierite Co., LTD, Ohio, USA) and flowed into a cavity ring-down spectrometer (CRDS; Picarro Inc., Santa Clara, CA, USA) to continuously measure the CO₂ and CH₄ concentrations. We ran the incubations for at least 30 min under light (200 μmol photons m⁻² s⁻¹) and dark conditions.

The concentration of CO₂ in the water circuit (μmol mL⁻¹) was calculated by Eq. (1):

$$[\text{CO}_2] = H^{\text{cp}} \times [\text{HP_CO}_2] \times (1 - p_{\text{H}_2\text{O}}), \quad (1)$$

where H^{cp} is the Henry constant (mol mL⁻¹ atm⁻¹) calculated using the *R* marelac package (Soetaert et al., 2016), [HP_CO₂] is the given concentration of CO₂ (ppm), and $p_{\text{H}_2\text{O}}$ is the water vapour pressure (atm).

The CO₂ fluxes were calculated from the change in CO₂ concentration over time during our incubations, correcting

for the seawater volume present in each core. Then, the fluxes were transformed to an aerial basis (μmol m⁻² h⁻¹) by taking into account the core surface area. Finally, the daily fluxes (μmol m⁻² d⁻¹) were calculated by multiplying the CO₂ flux obtained under light conditions by the number of light hours plus the CO₂ flux obtained under dark conditions by the number of dark hours.

The CH₄ fluxes were calculated in the same manner as for the CO₂ fluxes, with the exception that the Henry constant was calculated using Eq. (2):

$$\beta = H^{\text{cp}} \times (RT), \quad (2)$$

where H^{cp} is the Henry constant (mol mL⁻¹ atm⁻¹), R is the ideal gas constant (82.057338 atm mL mol⁻¹ K⁻¹), T is standard temperature (273.15 K), and β is the Bunsen solubility coefficient of CH₄, extracted from Wiesenburg and Guinasso (1979).

2.3.2 Measurement of CO₂ and CH₄ fluxes in sediment core incubations using the headspace technique

Mangrove sediment cores from stations S3 to S7 were incubated using a headspace technique in order to measure changes in CO₂ and CH₄ concentrations. Before starting the incubation, the seawater above the sediment from each core was replaced by fresh seawater from the running seawater system, leaving a headspace of 200 mL. Each core was sealed with a stopper equipped with a gas-tight valve serving as a headspace sampling port. The sealed core was left for 1 h before the first headspace sampling to allow equilibration between seawater and air phases. Each core was sampled with a syringe, withdrawing 15 mL of air from the equilibrated headspace. Headspace samples were periodically drawn from each sediment incubation over a 24 h incubation period. The CO₂ and CH₄ concentrations in the headspace samples along with their isotopic composition ($\delta^{13}\text{C-CO}_2$ and $\delta^{13}\text{C-CH}_4$) were measured with a CRDS (Picarro Inc., Santa Clara, CA, USA) connected to a small sample isotopic module extension (SSIM A0314, Picarro Inc., Santa Clara, CA, USA). We ran standards (730 ppm CO₂, 1.9 ppm CH₄) before and after every three samples.

The concentration of dissolved CO₂ in the seawater after equilibrium was calculated from the concentration in the equilibrated headspace (ppm) as described previously by Wilson et al. (2012) for other gases:

$$[\text{CO}_2]_{\text{w}} = 10^{-6} \beta m_{\text{a}} p_{\text{dry}}, \quad (3)$$

where β is the Bunsen solubility coefficient of CO₂ (mol mL⁻¹ atm⁻¹), m_{a} is the given concentration of CO₂ in the equilibrated headspace (ppm), and p_{dry} is atmospheric pressure (atm) of dry air. The Bunsen solubility coefficient of CO₂ was calculated using Eq. (4):

$$\beta = H^{\text{cp}} \times (RT), \quad (4)$$

where H^{cp} is the Henry constant ($\text{mol mL}^{-1} \text{atm}^{-1}$) calculated using the *R* marelac package (Soetaert et al., 2016), R is the ideal gas constant ($82.057338 \text{ atm mL mol}^{-1} \text{K}^{-1}$) and T is standard temperature (273.15 K). The atmospheric pressure of dry air (p_{dry}) was calculated using Eq. (5):

$$p_{\text{dry}} = p_{\text{wet}} (1 - \% \text{H}_2\text{O}), \quad (5)$$

where p_{wet} is the atmospheric pressure of wet air corrected by the effect of multiple syringe draws from the same core, applying Boyle's law.

The initial concentration of dissolved CO_2 in seawater before equilibrium was then calculated as follows:

$$[\text{CO}_2]_{\text{aq}} = \left([\text{CO}_2]_{\text{w}} V_{\text{w}} + 10^{-6} m_{\text{a}} V_{\text{a}} \right) / V_{\text{w}}, \quad (6)$$

where $[\text{CO}_2]_{\text{w}}$ is the concentration of dissolved CO_2 in the seawater after equilibrium, V_{w} is the volume of seawater (mL) and V_{a} is the headspace volume (mL) in the core. Finally, treating the gas as ideal, the units were converted to nM using Eq. (7):

$$[\text{CO}_2]_{\text{aq}} = 10^9 \times p_{\text{dry}} [\text{CO}_2]_{\text{aq}} / (RT), \quad (7)$$

where R is the ideal gas constant ($0.08206 \text{ atm L mol}^{-1} \text{K}^{-1}$) and T is temperature (K).

The CO_2 fluxes were calculated from the change in CO_2 concentration over time during our incubations, correcting for the seawater volume present in each core. Then, the fluxes were transformed to an aerial basis ($\mu\text{mol m}^{-2} \text{d}^{-1}$) by taking into account the core surface area. Finally, the day and night fluxes ($\mu\text{mol m}^{-2} \text{h}^{-1}$) were calculated from the change in CO_2 concentration between consecutive samplings during day and night-time.

The CH_4 fluxes were calculated in the same manner as the CO_2 fluxes, with the exception that the Bunsen solubility coefficient of CH_4 was calculated according to Wiesenburg and Guinasso (1979).

2.4 Isotopic composition of CO_2 ($\delta^{13}\text{C}-\text{CO}_2$) and CH_4 ($\delta^{13}\text{C}-\text{CH}_4$)

The isotopic signature of the CO_2 and CH_4 produced during incubations was estimated by conducting keeling plots (Pataki et al., 2003; Thom et al., 2003; Garcias-Bonet and Duarte, 2017). Briefly, the $\delta^{13}\text{C}$ of the CO_2 and CH_4 produced was extracted from the intercept of the linear regression between the inverse of the gas partial pressure and the isotopic signature. The data set is available from Sea et al. (2018).

3 Results

The mean ($\pm\text{SE}$) diel CO_2 and CH_4 emission rates for the seven sites were $372 \pm 1309 \mu\text{mol CO}_2 \text{ m}^{-2} \text{d}^{-1}$ and $5.6 \pm 1.6 \mu\text{mol CH}_4 \text{ m}^{-2} \text{d}^{-1}$ respectively. We observed high

Table 1. Summary of greenhouse gas fluxes and sediment characteristics from studied mangrove forests. CH_4 fluxes in brackets represent CO_2 equivalents in terms of global warming potential for a time horizon of 100 years (GWP_{100}), taking into account climate-carbon feedback as suggested by the AR5 of IPCC (Myhre et al., 2013). Data represent the mean \pm SEM and nd means no data available.

| Station | CO_2 Day flux ($\mu\text{mol CO}_2 \text{ m}^{-2} \text{h}^{-1}$) | CH_4 Day flux ($\mu\text{mol CH}_4 \text{ m}^{-2} \text{h}^{-1}$) | CO_2 Night flux ($\mu\text{mol CO}_2 \text{ m}^{-2} \text{h}^{-1}$) | CH_4 Night flux ($\mu\text{mol CH}_4 \text{ m}^{-2} \text{h}^{-1}$) | Daily CO_2 flux ($\mu\text{mol CO}_2 \text{ m}^{-2} \text{d}^{-1}$) | Daily CH_4 flux ($\mu\text{mol CH}_4 \text{ m}^{-2} \text{d}^{-1}$) | $\delta^{13}\text{C}-\text{CO}_2$ (%) | $\delta^{13}\text{C}-\text{CH}_4$ (%) | Nitrogen density (mgN cm^{-3}) | C _{org} density (mgC cm^{-3}) | $\text{Chl } a$ ($\mu\text{g Chl } a \text{ g}^{-1} \text{sediment}$) |
|---------|---|---|---|---|---|---|---------------------------------------|---------------------------------------|--|--|--|
| 1 | -188 ± 25 | 0.30 ± 0.17 [10.21] | -99 ± 18 | 0.19 ± 0.04 [6.46] | -3452 ± 271 | 5.9 ± 1.3 [20.11] | nd | nd | nd | nd | nd |
| 2 | -157 ± 89 | 0.05 ± 0.02 [1.71] | 782 ± 66 | 0.03 ± 0.01 [1.02] | 7500 ± 894 | 0.9 ± 0.25 [3.1] | nd | nd | 1.03 ± 0.05 | 13.33 ± 1.01 | nd |
| 3 | 49 ± 37 | 0.69 ± 0.4 [23.46] | -176 ± 23 | 0.42 ± 0.39 [14.28] | -1524 ± 686 | 13.3 ± 9.5 [45.2] | -25.7 ± 0.2 | -87.1 ± 2.3 | 0.80 ± 0.03 | 8.98 ± 0.86 | nd |
| 4 | -86 ± 79 | 0.28 ± 0.1 [9.52] | 29 ± 19 | 0.01 ± 0.03 [0.34] | -684 ± 1038 | 3.5 ± 0.8 [11.9] | -11.1 ± 0.6 | -71.3 ± 2.3 | 1.12 ± 0.05 | 13.34 ± 0.98 | 1.02 ± 0.05 |
| 5 | -22 ± 11 | 0.09 ± 0.03 [3.06] | 24 ± 20 | 0.13 ± 0.10 [4.42] | 23 ± 331 | 2.6 ± 1.6 [8.8] | -15.6 ± 2.3 | -83.6 ± 2.3 | 1.51 ± 0.14 | 10.58 ± 0.82 | 1.03 ± 0.04 |
| 6 | 73 ± 10 | 0.27 ± 0.10 [9.18] | 35 ± 17 | 0.45 ± 0.18 [15.30] | 1289 ± 280 | 8.7 ± 3.4 [29.6] | -12.9 ± 0.5 | -82.5 ± 1.7 | 3.30 ± 0.55 | 33.43 ± 6.69 | 0.43 ± 0.14 |
| 7 | -51 ± 28 | 0.13 ± 0.05 [4.42] | 5 ± 3 | 0.26 ± 0.03 [8.84] | -547 ± 363 | 4.6 ± 1.0 [15.6] | -15.9 ± 1.1 | -78.6 ± 0.6 | | | 1.86 ± 0.12 |

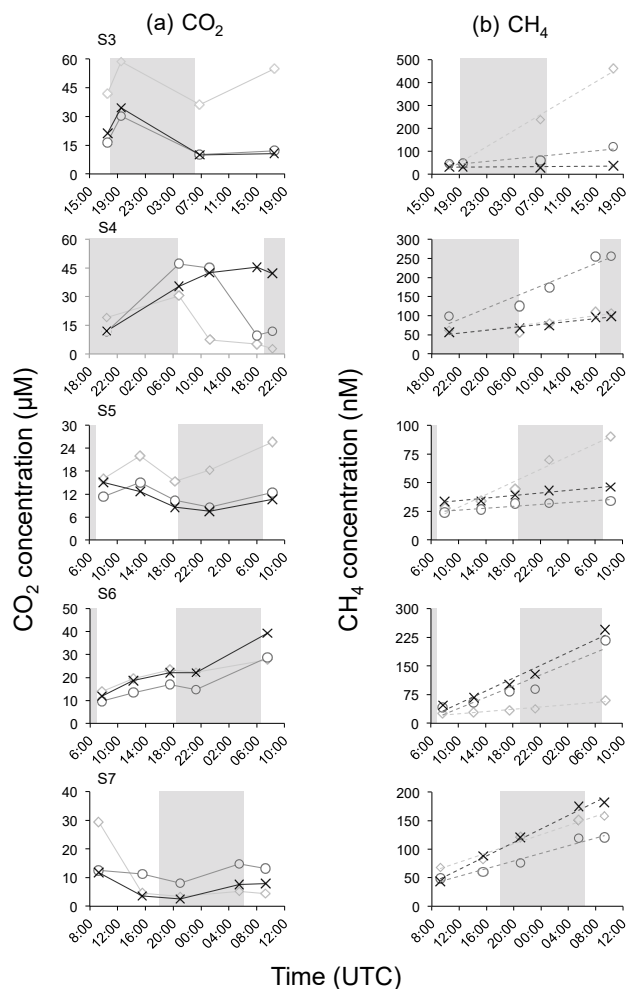


Figure 2. Change in CO₂ (a) and CH₄ (b) concentrations over time in triplicated mangrove sediment cores from mangrove stations S3–S7. Shaded areas represent night-time and each replicate is coded by different symbols.

variability among the seven mangrove forest sites studied, with net CO₂ and CH₄ diel emission rates ranging from -3452 to $7500 \mu\text{mol CO}_2 \text{ m}^{-2} \text{ d}^{-1}$ and from 0.9 to $13.3 \mu\text{mol CH}_4 \text{ m}^{-2} \text{ d}^{-1}$ (Table 1).

Mangrove sediments absorbed CO₂ during daytime and emitted CO₂ during night-time at 5 out of 7 stations, with means (\pm SE) of $-54.6 \pm 37 \mu\text{mol CO}_2 \text{ m}^{-2} \text{ h}^{-1}$ and $86 \pm 120 \mu\text{mol CO}_2 \text{ m}^{-2} \text{ h}^{-1}$ (Table 1, Fig. 2). However, in three out of seven sites, heterotrophic activities outbalanced photosynthesis on a 24 h basis. At two sites, S3 and S6, we found an increase of the CO₂ emissions between day and night, contradictory to the classical daytime primary production – night-time respiration pattern, possibly indicative of a light mediated increase in heterotrophic processes.

Methane emissions did not show circadian patterns with linear increases in CH₄ concentration in our incubations (Fig. 2) and with similar light and dark rates (0.26 ± 0.08 and

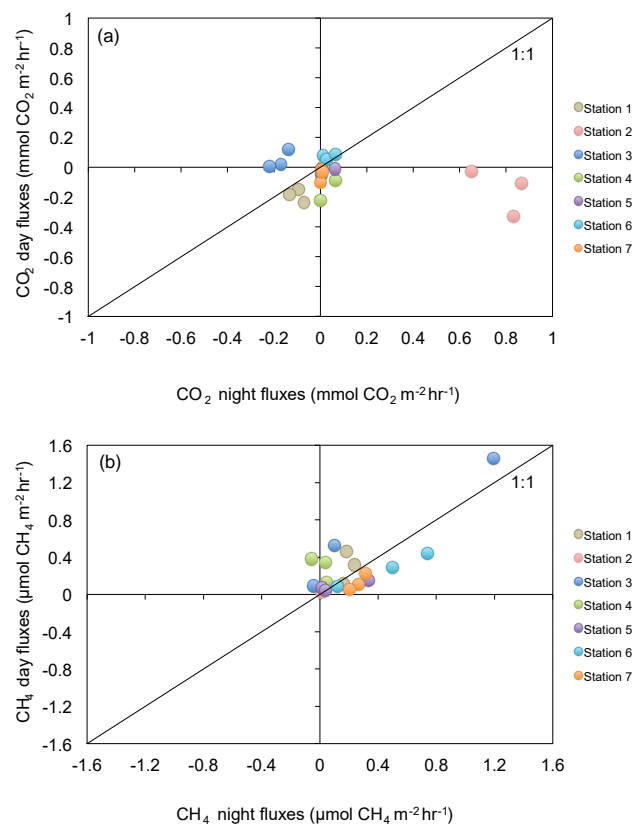


Figure 3. Relationship between day and night fluxes for CO₂ (a) and CH₄ (b) at all mangrove stations.

$0.21 \pm 0.07 \mu\text{mol CH}_4 \text{ m}^{-2} \text{ h}^{-1}$ (mean \pm SE) respectively; Table 1). In terms of the total GHG contribution, the mean CO₂ equivalent (CO₂e) emission to the atmosphere was $564 \pm 1284 \mu\text{mol CO}_2 \text{ e m}^{-2} \text{ d}^{-1}$ (mean \pm SE) using the 100-year time horizon global warming potential (Myhre et al., 2013). Inundated mangrove sediments were net emitters of CO₂e in three out of seven sites (Table 1), and in five out of seven mangrove stands sampled, CH₄ was the main source of CO₂e to the atmosphere.

While no overall trend was revealed through the relationship between day and night fluxes for CO₂ and CH₄ (Fig. 3), consistencies are evident at specific mangrove stations. For example, night CO₂ emissions are clearly visible at S2, while S3 appears to emit CO₂ during daylight hours. No relationship was apparent between GHG fluxes and the densities of organic carbon or nitrogen in the sediment. There was no discernible trend between gas fluxes and chlorophyll *a* content in surface sediments.

The isotopic signatures of the produced CO₂ ($\delta^{13}\text{C-CO}_2$) ranged from -11.21 to -25.72‰ as derived from keeling plots (Fig. 4, Table 1). The $\delta^{13}\text{C-CO}_2$ was similar for almost all stations, with the exception of S3, which had a $\delta^{13}\text{C-CO}_2$ of -25.72‰ . The isotopic composition of the produced CH₄

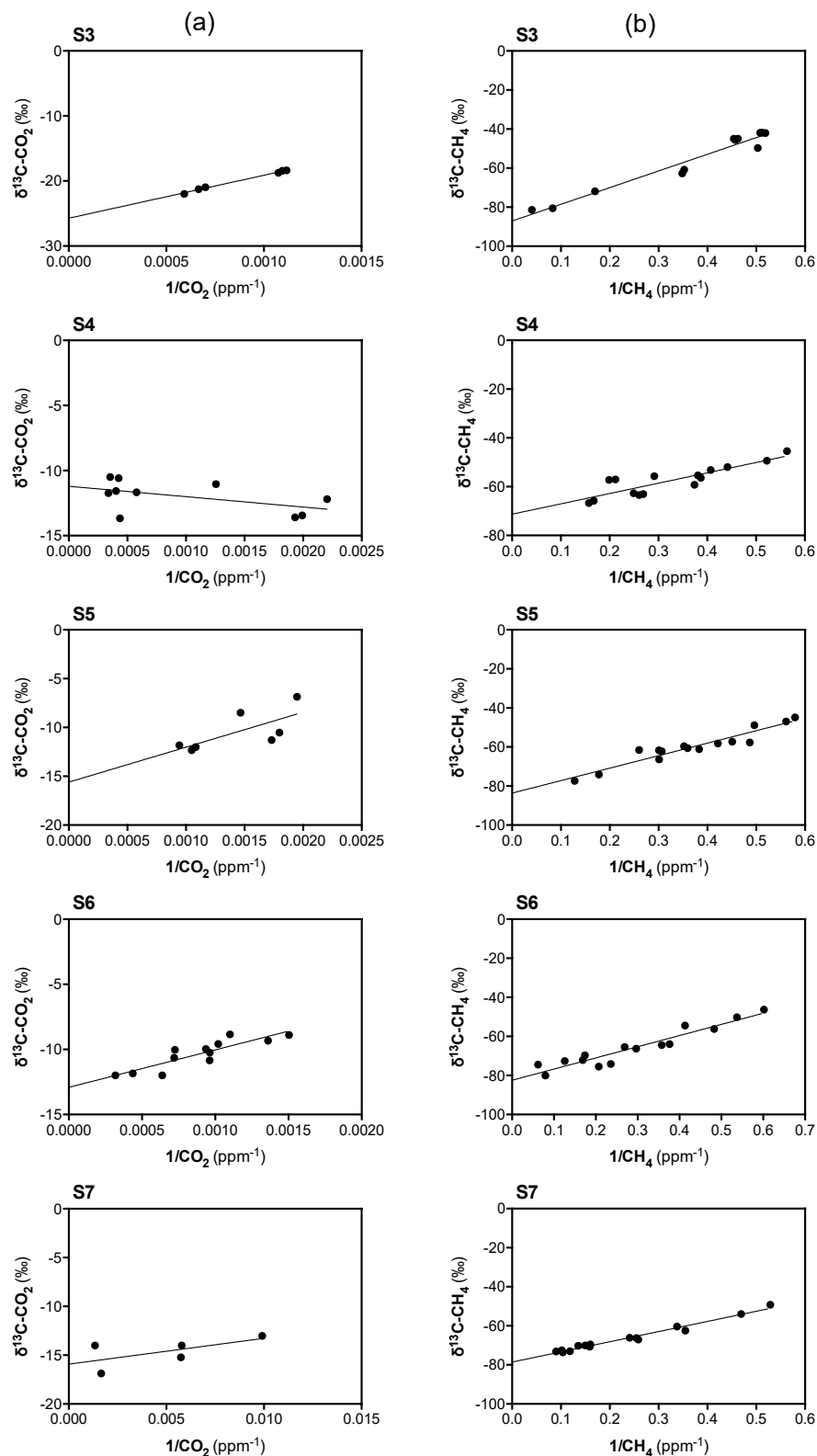


Figure 4. Keeling plots for mangrove stations S3–S7, showing the linear regression of the inverse of CO_2 concentration (a) and CH_4 concentration (b) versus $\delta^{13}\text{C}-\text{CO}_2$ and $\delta^{13}\text{C}-\text{CH}_4$. Y intercepts were used to estimate the isotopic signatures of produced gases.

($\delta^{13}\text{C-CH}_4$) ranged from -71.28 to -87.08‰ , with a mean $\delta^{13}\text{C}$ signature of -80.61‰ (Fig. 4, Table 1).

4 Discussion

4.1 Greenhouse gas fluxes

The CO_2 and CH_4 emissions reported in this study show that Red Sea mangroves can act as a source of GHG to the atmosphere. Values reported from this study fall within previously reported ranges for both CH_4 and CO_2 , but maximum CH_4 and CO_2 flux rates in the Red Sea are up to 100 fold below those reported elsewhere. Compiled global values for GHG fluxes range from -16.9 to $629.2\text{ mmol CO}_2\text{ m}^{-2}\text{ d}^{-1}$ and -2.1 to $25,974\text{ }\mu\text{mol CH}_4\text{ m}^{-2}\text{ d}^{-1}$, with mean ($\pm\text{SE}$) maximum emission rates averaging $202.3\pm 48\text{ mmol m}^{-2}\text{ d}^{-1}$ and $4783.6\pm 2783\text{ }\mu\text{mol m}^{-2}\text{ d}^{-1}$ for CO_2 and CH_4 respectively (Table 2).

The variability in GHG emission rates reported in this study could be attributed to spatial differences, as cores were taken from different parts of each forest. Indeed, previous studies report significant discrepancies in emission rates in fringe versus forest positions (Allen et al., 2007). Additionally it is possible that differences in flux rates may exist as a result of sediment disturbance from the coring process. The effects of mangrove pneumatophores and possible bioturbation from infaunal species such as burrowing crabs were not considered here yet could pose another possible source of variation in the results as the presence of these structures influences oxygenation of sediment and pore water exchange, identified as driving factors in varying CO_2 levels (Call et al., 2014; Rosentreter et al., 2018). These factors likely affect relevant redox processes and would therefore be useful to quantify in future studies.

Uniformity of day and night emission rates for CH_4 was observed in Red Sea mangrove stands, with mean ($\pm\text{SE}$) CH_4 emission rates of $0.28\pm 0.08\text{ }\mu\text{mol CH}_4\text{ m}^{-2}\text{ h}^{-1}$ during the day and $0.24\pm 0.08\text{ }\mu\text{mol CH}_4\text{ m}^{-2}\text{ h}^{-1}$ during night; this is consistent with previous work reporting that emission rates for CH_4 do not vary significantly during light and dark hours in mangrove forests (Allen et al., 2007). It has been suggested instead that variables such as sediment temperature are more significant in their contributions to emission rates (Allen et al., 2007, 2011). Incubated sediment cores kept at constant temperature do not reflect the range of temperatures experienced by mangrove sediments over the diurnal cycle; future studies examining GHG emissions under more realistic temperature fluctuations are needed. Seasonal studies of longer duration have reported increased emission rates during warmer seasons (Chen et al., 2016; Livesley and Andrusiak, 2012). Methane concentrations typically remain low due to anaerobic methane oxidation processes that take place near sediment surfaces (Kristensen et al., 2008a), consistent with the low CH_4 emission rates from Red Sea mangrove

sediments observed here. Additionally, environments of high salinity like the Red Sea have been associated with decreased CH_4 emissions, as sulfate-reducing bacteria are thought to outcompete methanogens (Poffenbarger et al., 2011).

Methane emission rates at the air–sea interface of Red Sea mangrove sediments, although quite low, become more substantial when considered in terms of global warming potential. In this study, CH_4 was, despite the comparatively low emission rates, the main source of CO_2e in the majority of sampled mangroves, and therefore deserves careful monitoring in this region. Reported organic carbon burial rates of Red Sea mangroves of $3.42\text{ mmol C m}^{-2}\text{ d}^{-1}$ (Almhasheer et al., 2017) are 10 times larger than the combined average CO_2 and CH_4 emission rates reported here ($0.37\text{ mmol C m}^{-2}\text{ d}^{-1}$), suggesting that these mangrove sediments could act as net atmospheric carbon sinks; however, significant alkalinity and DIC exports have been identified from mangroves as well (Sippo et al., 2016), necessitating future studies which measure these exports to neighbouring habitats in order to close the carbon budget and determine the role of Red Sea mangroves in potential climate change mitigation. Currently, protection measures and further reforestation efforts are being deployed along the Red Sea, which will further expand the area of mangroves (Almhasheer et al., 2016). The rationale for conserving mangroves in the climate change context is not adequately represented by their net carbon sink capacity when undisturbed, but rather by the emissions resulting from their disturbance. Indeed, previous studies analysing anthropogenic impacts on methane emission rates from mangrove sediments have shown that the a disturbance significantly increases methane emissions (Purvaja and Ramesh, 2001; Chen et al., 2011). This provides an additional rationale to conserve and continue to expand Red Sea mangroves.

While this study provides new insights into GHG fluxes from arid mangroves, the methods used here solely measure the air–sea fluxes of dissolved gases. If CO_2 is produced from underlying sediments, it enters the water column and becomes a part of the carbonate system, with the possibility of conversion to bicarbonate (HCO_3^-) and carbonate (CO_3^{2-}) ions; these dominating species represent over 99 % of the dissolved inorganic carbon (DIC) under current atmospheric and oceanic conditions (Zeebe and Wolf-Gladrow, 2001). Therefore, the air–sea equilibration methods used in this study do not measure DIC fluxes but only the fluxes of the dissolved CO_2 -component of this larger system.

Frankignoulle and Borges (2001) show that CO_2 can be measured either directly (using equilibrator techniques and spectroscopy or chromatography) or indirectly (by making calculations based on pH, total alkalinity, and DIC). The methodology presented in this study represents the former, utilizing an air–sea equilibrator connected to a CRDS to measure GHG fluxes at the air–sea interface. Research conducted by Borges et al. (2003) utilizes the indirect approach, using

Table 2. Comparison of GHG fluxes from global mangrove forests and Red Sea mangroves. Literature values converted from reported form for comparison purposes. Measurements made at the ¹ soil–atmosphere interface, ² air–sea interface with DIC calculation methods, and ³ air–sea interface with equilibration methods.

| Author | Year | Place | CO ₂ (mmol m ⁻² d ⁻¹) | | CH ₄ (μmol m ⁻² d ⁻¹) | |
|-------------------------------------|-------|------------------|---|---------|---|---------|
| | | | Minimum | Maximum | Minimum | Maximum |
| Allen et al. ¹ | 2007 | Australia | – | – | 4.5 | 25974 |
| Allen et al. ¹ | 2011 | Australia | – | – | 70.3 | 2348 |
| Alongi et al. ¹ | 2005 | China | 17 | 121 | 5 | 66 |
| Chen et al. ¹ | 2016 | China | –16.9 | 279.2 | –2.1 | 8015.1 |
| Kristensen et al. ^{1,2} | 2008b | Tanzania | 28 | 115 | 0 | 87.6 |
| Livesley and Andrusiak ¹ | 2012 | Australia | 50 | 150 | 50 | 749 |
| Borges et al. ² | 2003 | Papua New Guinea | – | 43.6 | – | – |
| Bouillon et al. ² | 2003 | India | – | 70.2 | – | – |
| Bouillon et al. ² | 2007a | Kenya | 3 | 252 | – | – |
| Bouillon et al. ² | 2007b | Kenya | – | 52 | – | – |
| Bouillon et al. ² | 2007c | Tanzania | 1 | 80 | – | – |
| Call et al. ³ | 2015 | Australia | 9.4 | 629.2 | 13.1 | 632.9 |
| Ho et al. ³ | 2014 | United States | 20 | 118 | – | – |
| Jacotot et al. ³ | 2018 | New Caledonia | 3.12 | 441.8 | 4.32 | 4129.7 |
| Rosentreter et al. ³ | 2018a | Australia | 58.7 | 277.6 | – | – |
| Rosentreter et al. ³ | 2018b | Australia | – | – | 96.5 | 1049.8 |
| This Study ³ | 2017 | Red Sea | –3.5 | 7.5 | 0.9 | 13.3 |

pH and total alkalinity measurements in Papua New Guinea to calculate DIC and CO₂(dis) (for a computational discussion see Frankignoulle and Borges, 2001). Both methods measure at the air–sea interface (Table 2) but are not directly comparable, as a full determination of the carbonate system was not carried out in the present study. Similarly, studies using equilibrator techniques that measure the dissolved CO₂ fraction of seawater to the atmosphere are influenced by the seawater carbonate system and further steps of isotopic fractionation (discussed below) and are therefore not directly comparable to those studies which measure GHG fluxes from exposed mangrove sediments to the atmosphere (Table 2).

4.2 Isotopic composition of emitted gases

There were no relationships between GHG fluxes and sediment properties, such as chlorophyll *a*, nitrogen density, and organic carbon density, suggesting that other factors have a greater influence on GHG flux rates in this region. Since mangroves can receive large contributions of organic carbon from other sources (Newell et al., 1995), such as algal mats, seagrass and seaweed, examination of the isotopic composition of emitted carbon provides insights into the origin of the organic carbon supporting GHG fluxes in mangrove sediments; however, it should be noted that δ¹³C values reported in this study occur after several steps of isotopic fractionation and may therefore influence results. Isotope effects can cause an unequal distribution of isotopes between DIC components; for example, as CO₂ is produced from mangrove

sediments and becomes part of the carbonate system (likely forming HCO₃⁻ after equilibration), molecules containing the heavier carbon isotope – with a higher activation energy – will typically react more slowly (Zeebe and Wolf-Gladrow, 2001), promoting a higher concentration of the heavy isotope in unreacted CO₂ and a relative depletion of this heavier isotope in resulting HCO₃⁻. Similarly, this preferential incorporation and movement of molecules containing lighter isotopes can affect resulting carbon isotope ratios after air–sea equilibration (with depletion of lighter isotopes in seawater as a result of fractionation). CO₂ measured in this study is subject to these processes and may not reflect the isotopic ratios of carbon originally emitted; rather, the signatures measured in this study should be seen as a proxy which reflects isotopic ratios of air–sea discrimination and biological processing (decomposition, respiration, and photosynthesis), resulting after carbon isotope fractionation. An interpretation of the results is therefore subject to this limitation.

The isotopic signature of the CO₂ (δ¹³C-CO₂) produced by mangrove sediments in four out of the five mangrove stands with available isotopic data was heavier (from –11.2 ± 0.6 to –15.9 ± 1.1‰; Table 1) than the isotopic signature of mangrove tissues, suggesting decomposition of organic matter from mixed sources (Kennedy et al., 2010). Specifically, the isotopic signature of the mangroves found in the central Red Sea has been recently reported as δ¹³C_{leaves} = –26.98 ± 0.15‰, δ¹³C_{stems} = –25.75 ± 0.16 and δ¹³C_{roots} = –24.90 ± 0.17‰ for mangrove leaves, stems and roots, while the mean isotopic signature of other pri-

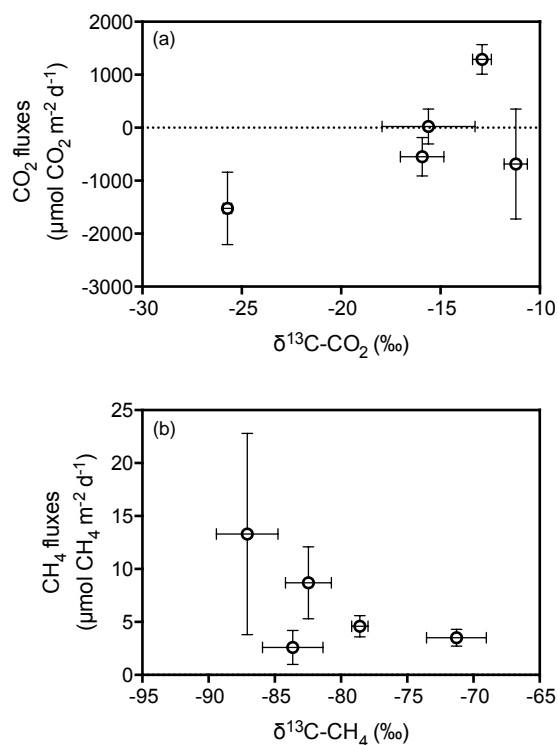


Figure 5. Relation between (a) the carbon isotopic signature of the produced CO₂ (δ¹³C-CO₂) and CO₂ fluxes and (b) carbon isotopic signature of the produced CH₄ (δ¹³C-CH₄) and the CH₄ fluxes in Red Sea mangroves. Error bars indicate standard error of the mean.

mary producers in the central Red Sea has been reported as $\delta^{13}\text{C}_{\text{seaweed}} = -12.8 \pm 0.5$ and $\delta^{13}\text{C}_{\text{seagrass}} = -8.2 \pm 0.2$ ‰ for seaweed and seagrass tissues respectively (Almahasheer et al., 2017). However, in one mangrove stand (S3) the $\delta^{13}\text{C-CO}_2$ was much lighter (-25.72 ± 0.21 ‰), potentially indicating mangrove tissues. Thus, according to the isotopic signature, the CO₂ produced in mangrove sediments would be supported by mangrove biomass in only one mangrove stand out of the five sampled sites with available isotopic data. Moreover, the mean isotopic signature of the CH₄ produced in mangrove sediments ($\delta^{13}\text{C-CH}_4 = -80.6$ ‰) tentatively confirms its biogenic origin, which normally ranges from -40 to -80 ‰, depending on the isotopic signature of the organic compounds being biologically decomposed (Reeburgh, 2014). The lowest $\delta^{13}\text{C-CH}_4$ was detected in S3, coinciding with the lowest $\delta^{13}\text{C-CO}_2$ value, suggesting that the organic matter being decomposed by methanogens likely came from mangrove tissues as well.

Interestingly, the mangrove with the lightest $\delta^{13}\text{C-CO}_2$ and $\delta^{13}\text{C-CH}_4$ (S3) showed the lowest daily CO₂ flux (-1524 ± 686 μmol CO₂ m⁻² d⁻¹) but the highest CH₄ emission rate (13.3 ± 9.5 μmol CH₄ m⁻² d⁻¹) compared to the fluxes detected in the rest of mangrove stands with available isotopic data. Part of the variability in the CO₂ ($R^2 = 0.42$)

and CH₄ ($R^2 = 0.40$) emission rate seems to be explained by the origin of the organic matter being decomposed, estimated here as $\delta^{13}\text{C-CO}_2$ and $\delta^{13}\text{C-CH}_4$. Organic matter with lighter isotopic composition could enhance CO₂ emissions, whereas organic matter with heavier isotopic composition could enhance CH₄ emissions (Fig. 5), possibly suggesting a different preferential use of organic matter by different microbial groups in mangrove sediments. Future studies exploring this idea with further considerations of carbon isotope fractionation would help solidify the role of the origin of organic carbon stored in mangrove sediments on their GHG emissions.

5 Conclusions

This study is first in reporting CO₂ and CH₄ fluxes from Red Sea mangrove sediments, contributing to the scant data on arid mangrove systems (Atwood et al., 2017; Almahasheer et al., 2017), essential to establishing a solid baseline on GHG emissions for future studies. Results show that maximum CO₂ and CH₄ flux rates from Red Sea mangrove sediments are well below those reported elsewhere, and that, even when considered in terms of CO₂ equivalents, carbon burial rates largely outweigh GHG emission rates at the air–sea interface in this region. This study also highlights the importance of determining the source of organic matter in GHG flux studies, as emissions appear to be supported by organic matter from mixed sources in the majority of studied mangroves, potentially enhancing CH₄ production over CO₂ fluxes in this system. Seasonal variation should be considered in future studies on GHG emissions by Red Sea mangroves to better determine annual emission rates from this system, which reach some of the warmest temperatures experienced by mangrove forests worldwide. Similarly, a wider spatial coverage within the mangrove forest should be considered to confidently determine net GHG fluxes that can be upscaled to the entire stock of Red Sea mangroves.

Methods presented in this study include the use of an air–sea equilibrator connected to a CRDS to measure GHG fluxes at the air–sea interface, measuring the dissolved CO₂ component of the larger seawater carbonate system. This methodology is one of many used to measure GHG flux rates; establishing a unified sampling technique at both the soil–atmosphere and air–seawater interface will aid future researchers in determining total carbon budgets and accurately informing policymakers of their findings. In combination with a consideration of isotope effects, a full determination of the carbonate system will be beneficial in future studies to further resolve GHG fluxes in arid mangroves, allowing us to better ascertain the role of these forests in global carbon budgets.

Data availability. All data will be accessible in the repository Pangea (<https://doi.org/10.1594/PANGAEA.892847>; Sea et al., 2018)

Author contributions. MAS, NGB, VS, and CMD designed the study. MAS and NGB made the measurements and calculations. MAS, NGB, VS, and CMD interpreted the results. All authors contributed substantially to the final manuscript.

Competing interests. The authors declare that they have no conflict of interest.

Acknowledgements. This research was funded by King Abdullah University of Science and Technology (KAUST) through baseline funding to Carlos M. Duarte. We thank Dorte Krause-Jensen, Nadia Salah Massoudi Ennasri, and Kimberly Baldry for help during sampling, and the captain and crew of KAUST R/V *Thuwal* for support. Mallory A. Sea was supported by King Abdullah University of Science and Technology through the VRSP programme. We thank Paloma Carrillo de Albornoz for lab instrument support, and Mongi Ennasri for help with sediment analysis.

Edited by: Caroline P. Slomp

Reviewed by: two anonymous referees

References

- Allen, D. E., Dalal, R. C., Rennenberg, H., Meyer, R., L., Reeves, S., and Schmidt, S.: Spatial and temporal variation of nitrous oxide and methane flux between subtropical mangrove sediments and the atmosphere, *Soil. Biol. Biochem.*, 39, 622–631, 2007.
- Allen, D. E., Dalal, R. C., Rennenberg, H., and Schmidt, S.: Seasonal variation in nitrous oxide and methane emissions from subtropical estuary and coastal mangrove sediments, *Australia. Plant. Biol.*, 13, 126–133, 2011.
- Almahasheer, H., Aljowair, A., Duarte, C. M., and Irigoien, X.: Decadal stability of Red Sea mangroves, *Estuar. Coast. Shelf. S.*, 169, 164–172, 2016.
- Almahasheer, H., Serrano, O., Duarte, C. M., Arias-Ortiz, A., Masque, P., and Irigoien, X.: Low carbon sink capacity of Red Sea mangroves, *Sci. Rep.*, 7, 9700, <https://doi.org/10.1038/s41598-017-10424-9>, 2017.
- Alongi, D. M.: Mangrove forests: Resilience, protection from tsunamis, and responses to global climate change, *Estuar. Coast. Shelf. S.*, 76, 1–13, 2008.
- Alongi, D. M.: Carbon sequestration in mangrove forests, *Carbon. Manag.*, 3, 313–322, <https://doi.org/10.4155/cmt.12.20>, 2012.
- Alongi, D. M.: Carbon cycling and storage in mangrove forests, *Annu. Rev. Mar. Sci.*, 6, 195–219, <https://doi.org/10.1146/annurev-marine-010213-135020>, 2014.
- Alongi, D. M., Pfitzner, J., Trott, L. A., Tirendi, F., Dixon, P., and Klumpp, D. W.: Rapid sediment accumulation and microbial mineralization in forests of the mangrove *Kandelia candel* in the Jiulongjiang Estuary, China, *Estuar. Coast. Shelf. S.*, 63, 605–618, 2005.
- Atwood, T. B., Connolly, R. M., Almahasheer, H., Carnell, P., Duarte, C. M., Ewers, C., Irigoien, X., Kelleway, J., Lavery, P. S., Macreadie, P. I., Serrano, O., Sanders, C., Santos, I., Steven, A., and Lovelock, C. E.: Global patterns in mangrove soil carbon stocks and losses, *Nat. Clim. Change*, 7, 523–529, <https://doi.org/10.1038/nclimate3326>, 2017.
- Borges, A. V., Djenidi, S., Lacroix, G., Theate, J., Delille, B., and Frankignoulle, M.: Atmospheric CO₂ flux from mangrove surrounding waters, *Geophys. Res. Lett.*, 30, 1558, <https://doi.org/10.1029/2003GL017143>, 2003.
- Bouillon, S., Frankignoulle, M., Dehairs, F., Velimirov, B., Eiler, A., Gwenael, A., Etcheber, H., and Borges, A. V.: Inorganic and organic carbon biogeochemistry in the Gautami Godavari estuary (Andhra Pradesh, India) during pre-monsoon: The local impact of extensive mangrove forests, *Global Biogeochem. Cy.*, 17, 1114, <https://doi.org/10.1029/2002GB002026>, 2003.
- Bouillon, S., Dehairs, F., Schiettecatte, L., and Alberto Vieira Borges, A. V.: Biogeochemistry of the Tana estuary and delta (northern Kenya), *Limnol. Oceanogr.*, 52, 46–59, 2007a.
- Bouillon, S., Dehairs, F., Velimirov, B., Gwenael, A., and Borges, A. V.: Dynamics of organic and inorganic carbon across contiguous mangrove and seagrass systems (Gazi Bay, Kenya), *J. Geophys. Res.*, 112, G02018, <https://doi.org/10.1029/2006JG000325>, 2007b.
- Bouillon, S., Middelburg, J. J., Dehairs, F., Borges, A. V., Abril, G., Flindt, M. R., Ulomi, S., and Kristensen, E.: Importance of intertidal sediment processes and porewater exchange on the water column biogeochemistry in a pristine mangrove creek (Ras Dege, Tanzania), *Biogeosciences*, 4, 311–322, <https://doi.org/10.5194/bg-4-311-2007>, 2007c.
- Call, M., Maher, D. T., Santos, I. R., Ruiz-Halpern, S., Mangion, P., Sanders, C. J., Erler, D. V., Oakes, J. M., Rosentreter, J., Murray, R., and Eyre, B. D.: Spatial and temporal variability of carbon dioxide and methane fluxes over semi-diurnal and spring-neap-spring timescales in a mangrove creek, *Geochim. Cosmochim. Ac.*, 150, 211–225, 2015.
- Chauhan, R., Datta, A., Ramanathan, A. L., and Adhya, T. K.: Factors influencing spatio-temporal variation of methane and nitrous oxide emission from a tropical mangrove of eastern coast of India, *Atmos. Environ.*, 107, 95–106, 2015.
- Chen, G., Tam, N. F. Y., Wong, Y. S., and Ye, Y.: Effect of wastewater discharge on greenhouse gas fluxes from mangrove soils, *Atmos. Environ.*, 45, 1110–1115, 2011.
- Chen, G., Chen, B., Yu, D., Tam, N. F. Y., Ye, Y., and Chen, S.: Soil greenhouse gas emissions reduce the contribution of mangrove plants to the atmospheric cooling effect, *Environ. Res. Lett.*, 11, 1–10, <https://doi.org/10.1088/1748-9326/11/12/124019>, 2016.
- Duarte, C. M., Losada, I. J., Hendriks, I. E., Mazarrasa, I., and Marbà, N.: The role of coastal plant communities for climate change mitigation and adaptation, *Nat. Clim. Change*, 3, 961–968, <https://doi.org/10.1038/NCLIMATE1970>, 2013.
- Donato, D. C., Kauffman, J. B., Murdiyarso, D., Kurnianto, S., Stidham, M., and Kanninen, M.: Mangroves among the most carbon-rich forests in the tropics, *Nat. Geosci.*, 4, 293–297, <https://doi.org/10.1038/NCEO1123>, 2011.
- Frankignoulle, M. and Borges, A. V.: Direct and indirect pCO₂ measurements in a wide range of pCO₂ and salinity values (the Scheldt Estuary), *Aquat. Geochem.*, 7, 267–273, 2001.

- Garcias-Bonet, N. and Duarte, C. M.: Methane production by seagrass ecosystems in the Red Sea, *Front. Mar. Sci.*, 4, 1–10, <https://doi.org/10.3389/fmars.2017.00340>, 2017.
- Giri, C., Ochieng, E., Tieszen, L. L., Zhu, Z., Singh, A., Loveland, T., Masek, J., and Duke, N.: Status and distribution of mangrove forests of the world using earth observation satellite data, *Global Ecol. Biogeogr.*, 20, 154–159, 2011.
- Ho, D. T., Ferrón, S., Engel, V. C., Larsen, L. G., and Barr, J. G.: Air-water gas exchange and CO₂ flux in a mangrove-dominated estuary, *Geophys. Res. Lett.*, 41, 108–113, <https://doi.org/10.1002/2013GL058785>, 2014.
- Jacotot, A., Marchand, C., and Allenbach, M.: Tidal variability of CO₂ and CH₄ emissions from the water column within a Rhizophora mangrove forest (New Caledonia), *Sci. Total. Environ.*, 631, 334–340, 2018.
- Kennedy, H., Beggins, J., Duarte, C. M., Fourqurean, J. W., Holmer, M., Marbà, N., and Middelburg, J. J.: Seagrass sediments as a global carbon sink: isotopic constraints, *Global Biogeochem. Cy.*, 24, GB4026, <https://doi.org/10.1029/2010GB003848>, 2010.
- Kristensen, E., Bouillon, S., Dittmar, T., and Marchand, C.: Organic carbon dynamics in mangrove ecosystems: A review, *Aquat. Bot.*, 89, 201–219, <https://doi.org/10.1016/j.aquabot.2007.12.005>, 2008a.
- Kristensen, E., Flindt, M. R., Ulomi, S., Borges, A. V., Abril, G., and Bouillon, S.: Emissions of CO₂ and CH₄ to the atmosphere by sediments and open waters in two Tanzanian mangrove forests, *Mar. Ecol. Prog. Ser.*, 370, 53–67, <https://doi.org/10.3354/meps07642>, 2008b.
- Livesley, S. J. and Andrusiak, S. M.: Temperate mangrove and salt marsh sediments are a small methane and nitrous oxide source but important carbon store, *Estuar. Coast. Shelf. Sci.*, 97, 19–27, 2012.
- Myhre, G., Shindell, D., Bréon, F. M., Collins, W., Fuglestedt, J., Huang, J., Koch, D., Lamarque, J. F., Lee, D., Mendoza, B., and Nakajima, T.: Anthropogenic and natural radiative forcing, *Climate Change*, 423, 658–740, 2013.
- Newell, R. I. E., Marshall, N., Sasekumar, A., and Chong, V. C.: Relative importance of benthic microalgae, phytoplankton, and mangroves as sources of nutrition for penaeid prawns and other coastal invertebrates from Malaysia, *Mar. Biol.*, 123, 595–606, 1995.
- Pataki, D., Ehleringer, J. R., Flanagan, L. B., Yakir, D., Bowling, D. R., Still, C. J., Buchmann, N., Kaplan, J. O., and Berry, J. A.: The application and interpretation of Keeling plots in terrestrial carbon cycle research, *Global Biogeochem. Cy.*, 17, 1022, <https://doi.org/10.1029/2001GB001850>, 2013.
- Poffenbarger, H. J., Needelman, B. A., and Megonigal, J. P.: Salinity influence on methane emissions from tidal marshes, *Wetlands*, 31, 831–842, <https://doi.org/10.1007/s13157-011-0197-0>, 2011.
- Purvaja, R. and Ramesh, R.: Human impacts on methane emission from mangrove ecosystems in India, *Reg. Environ. Change*, 1, 86–97, <https://doi.org/10.1007/PL00011537>, 2000.
- Purvaja, R. and Ramesh, R.: Natural and anthropogenic methane emission from wetlands of south India, *Environ. Manage.*, 27, 547–557, <https://doi.org/10.1007/s002670010169>, 2001.
- Reeburgh, W. S.: *Global Methane Biogeochemistry Treatise on Geochemistry*, 2nd Edn., edited by: Holland, H. D. and Turekian, K. K., Oxford, Elsevier, 71–94, 2014.
- Rosentreter, J. A., Maher, D. T., Erler, D. V., Murray, R., and Eyre, B. D.: Seasonal and temporal CO₂ dynamics in three tropical mangrove creeks – A revision of global mangrove CO₂ emissions, *Geochim. Cosmochim. Ac.*, 222, 729–745, 2018a.
- Rosentreter, J. A., Maher, D. T., Erler, D. V., Murray, R. H., and Eyre, B. D.: Methane emissions partially offset “blue carbon” burial in mangroves, *Sci. Adv.*, 4, eaao4985, <https://doi.org/10.1126/sciadv.aao4985>, 2018b.
- Sea, M. A., Garcias-Bonet, N., Saderne, V., and Duarte, C. M.: Data set on methane emissions from Red Sea mangrove sediments, Pangea, available at: 10.1594/PANGAEA.892847, last access: 21 August 2018.
- Sippo, J. Z., Maher, D. T., Tait, D. R., Holloway, C., and Santos, I. R.: Are mangroves drivers or buffers of coastal acidification? Insights from alkalinity and dissolved inorganic carbon export estimates across a latitudinal transect, *Global Biogeochem. Cy.*, 30, 753–766, 2016.
- Soetaert, K., Petzoldt, T., and Meysman, F.: Marelac: A tool for aquatic sciences (R package), available at: <https://cran.r-project.org/web/packages/marelac/marelac.pdf> (3 June 2018), 2016.
- Thom, M., Bosinger, R., Schmidt, M., and Levin, I.: The regional budget of atmospheric methane of a highly populated area, *Chemosphere*, 26, 143–160, [https://doi.org/10.1016/0045-6535\(93\)90418-5](https://doi.org/10.1016/0045-6535(93)90418-5), 1993.
- Wiesenburg, D. A. and Guinasso, N. L.: Equilibrium solubilities of methane, carbon monoxide, and hydrogen in water and sea water, *J. Chem. Eng. Data*, 24, 356–360, 1979.
- Wilson, S. T., Böttjer, D., Church, M. J., and Karla, D. M.: Comparative assessment of nitrogen fixation methodologies, conducted in the oligotrophic north Pacific Ocean, *Appl. Environ. Microb.*, 78, 6516–6523, 2012.
- Zeebe, R. E. and Wolf-Gladrow, D. A.: CO₂ in seawater: equilibrium, kinetics, isotopes, Elsevier, Amsterdam, 2001.